Electronic Supplementary Material (ESI) for Physical Chemistry Chemical Physics.

Supplementary Information of

Exoergic pathways triggered by O/H radicals in different metallic carbohydrazide perchlorates (M^{2+}= Mn^{2+}, Fe^{2+}, Co^{2+}, Ni^{2+}, Zn^{2+} and Cd^{2+})

Xiaohui He ,‡[a] Panpan Wu, ‡[a] Xin Huang,[a] Chaohua Dai,[a] Changshun Li,[a] Longjiu Cheng,[a] Tonglai Zhang,*[c] Jianguo Zhang*[c] and Kun Wang *[a,b]

[a]*Department of Chemistry, Anhui University, Hefei, Anhui 230601, P. R. China*

[b]*Key Laboratory of Structure and Functional Regulation of Hybrid Materials (Anhui University), Ministry of Education; Hefei, Anhui 230601, P. R. China*

[c]*State Key Laboratory of Explosion Science and Technology, Beijing Institute of Technology, Beijing 100081 P. R. China*

‡*These two authors contributed equally to this work.*

* Corresponding authors: Kun Wang, Tel & Fax: +86 551 63861279. E-mail: wangkun@ahu.edu.cn; Tonglai Zhang, E-mail: ztlbit@bit.edu.cn; Jianguo Zhang, E-mail: zjgbit@bit.edu.cn

Contents

To satisfy the requirements of the simulation, we test the virtual mass of electronics and the cut off energy to make sure the systems are adiabatic with appropriate force fields for all the atoms before increasing the temperature. The average value of the temperature of ions (T_{ion}), kinetic energies of virtual electrons (e_{kinc}) and the total electronic energies (e_{tot}) in a 2000-step simulation without any thermostat (Table S10 ~ S14).

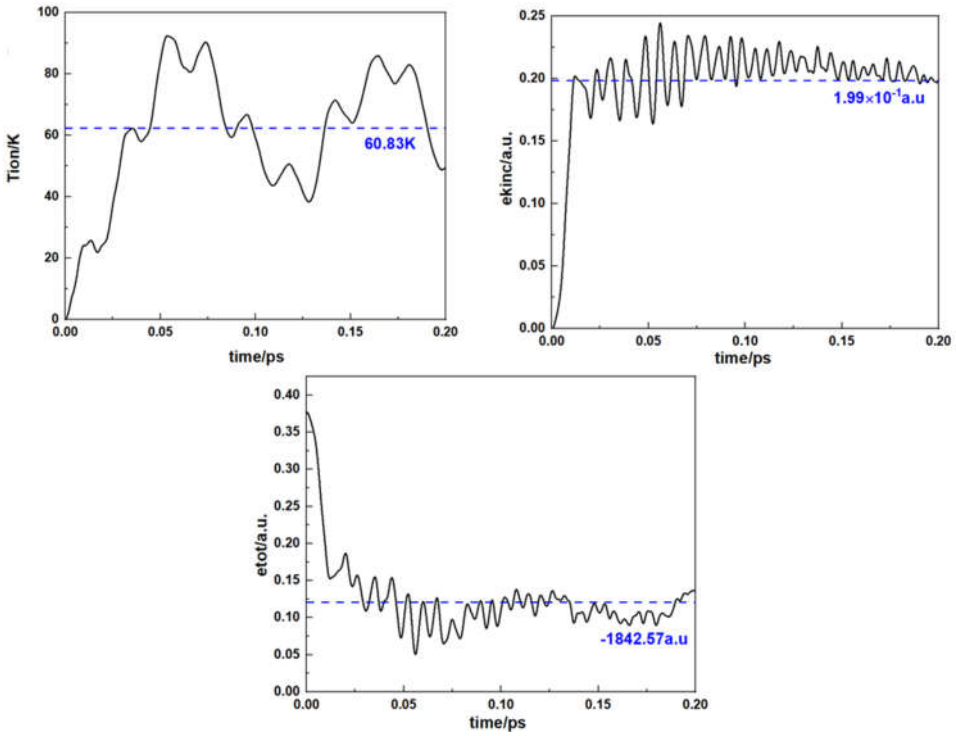

Fig. S1. The convergence curves of the temperature of ions (T_{ions}), kinetic energies of virtual electrons (e_{kinc}) and the total electronic energies (e_{tot}) of MnCP

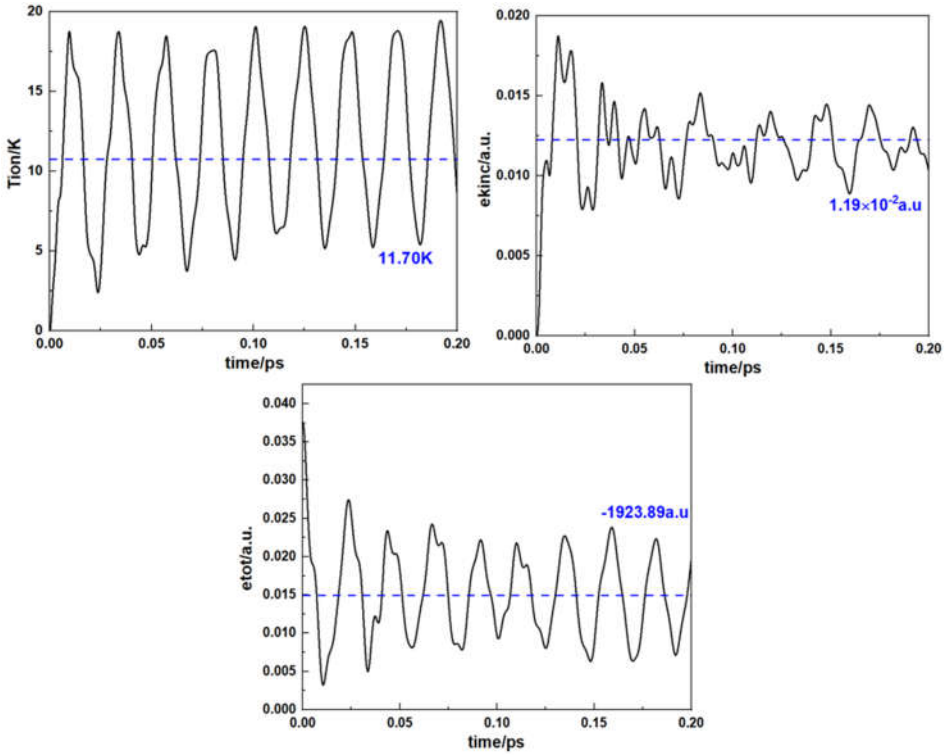

Fig. S2. The convergence curves of the temperature of ions (T_{ions}), kinetic energies of virtual electrons (e_{kinc}) and the total electronic energies (e_{tot}) of FeCP

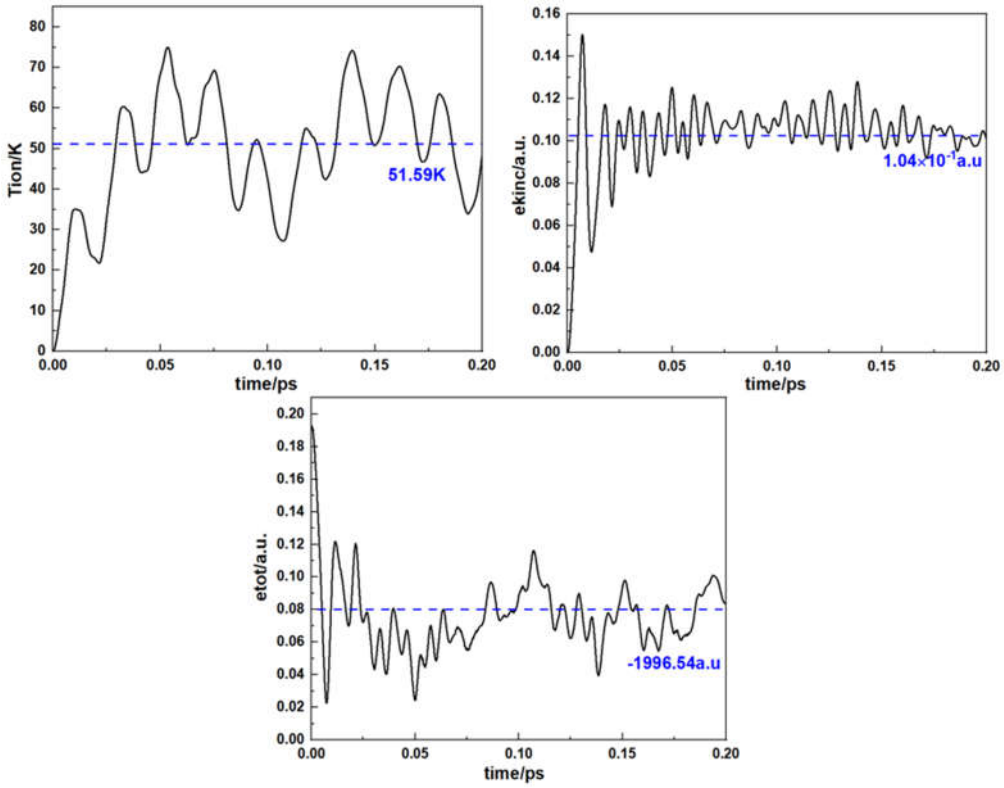

Fig. S3. The convergence curves of the temperature of ions (T_{ions}), kinetic energies of virtual electrons (e_{kinc}) and the total electronic energies (e_{tot}) of CoCP

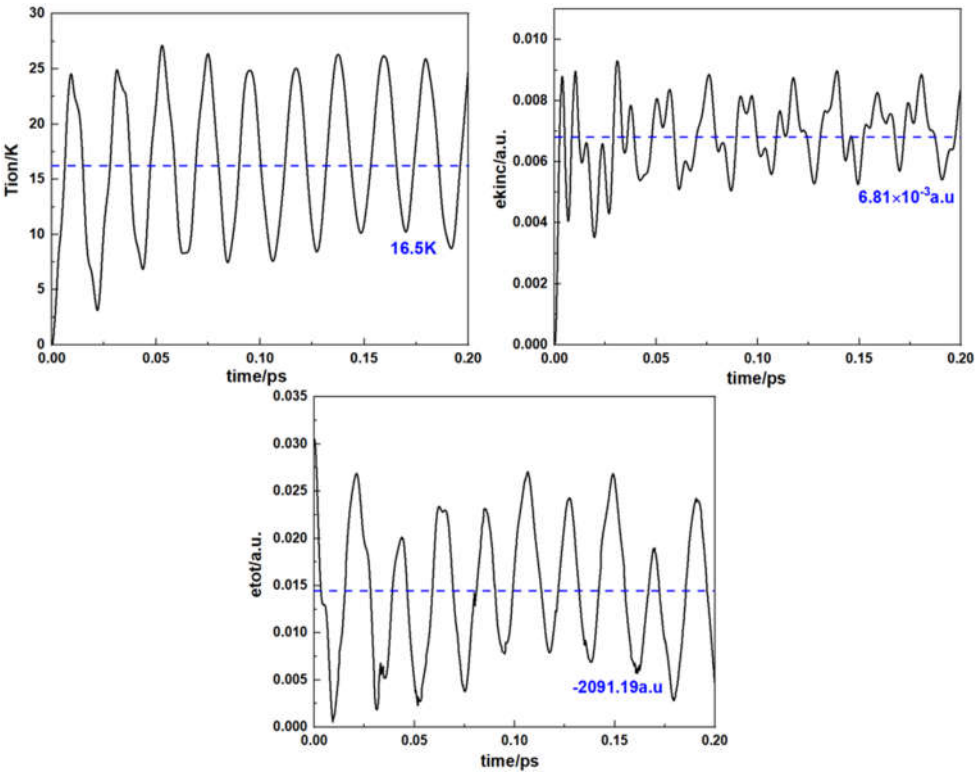

Fig. S4. The convergence curves of the temperature of ions (T_{ions}), kinetic energies of virtual electrons (e_{kinc}) and the total electronic energies (e_{tot}) of NiCP

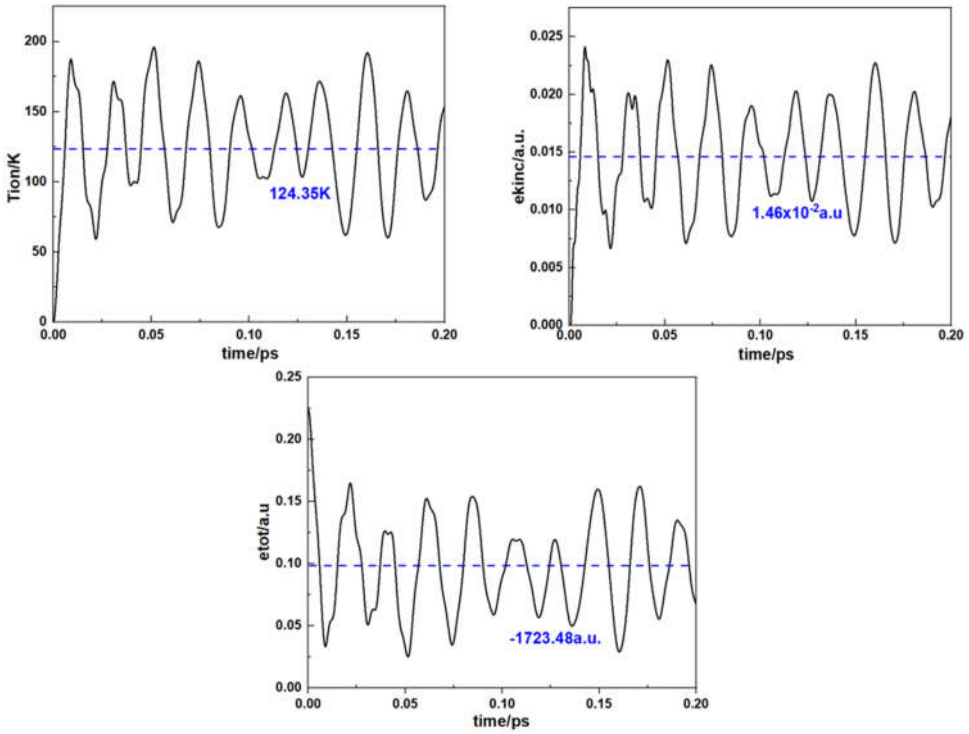

Fig. S5. The convergence curves of the temperature of ions (T_{ions}), kinetic energies of virtual electrons (e_{kinc}) and the total electronic energies (e_{tot}) of FeCP

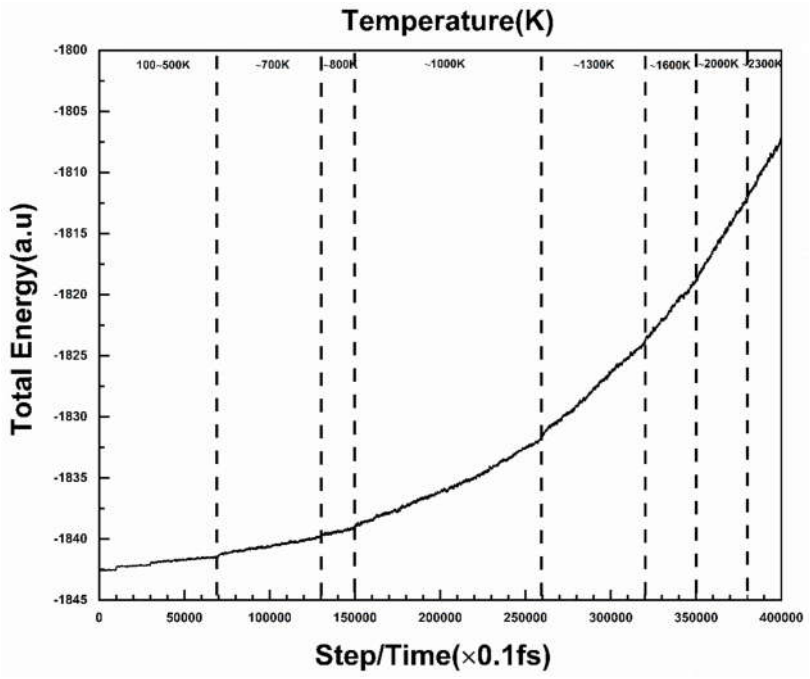

Fig. S6. The relationship between the total energy and the simulation time/temperature of MnCP

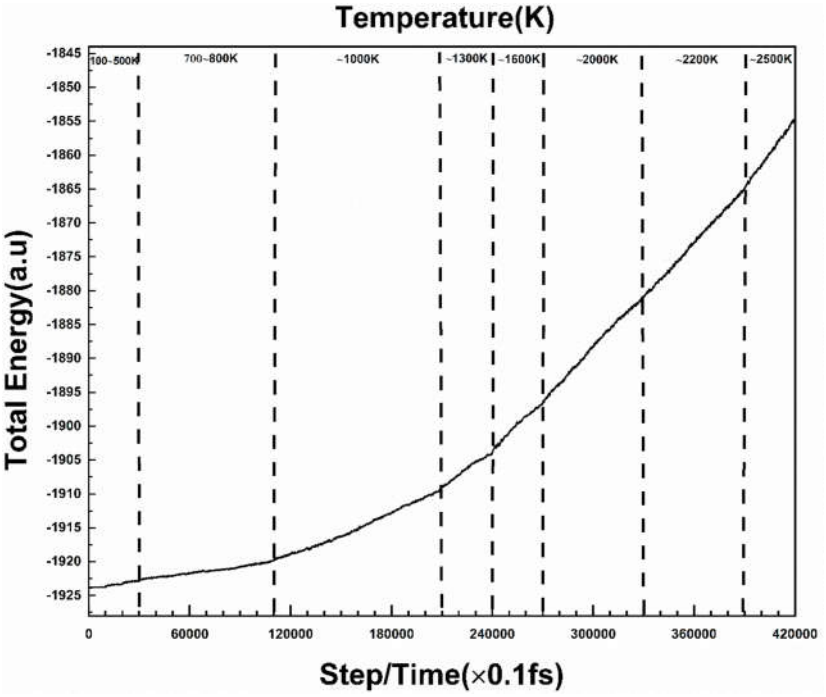

Fig. S7. The relationship between the total energy and the simulation time/temperature of FeCP

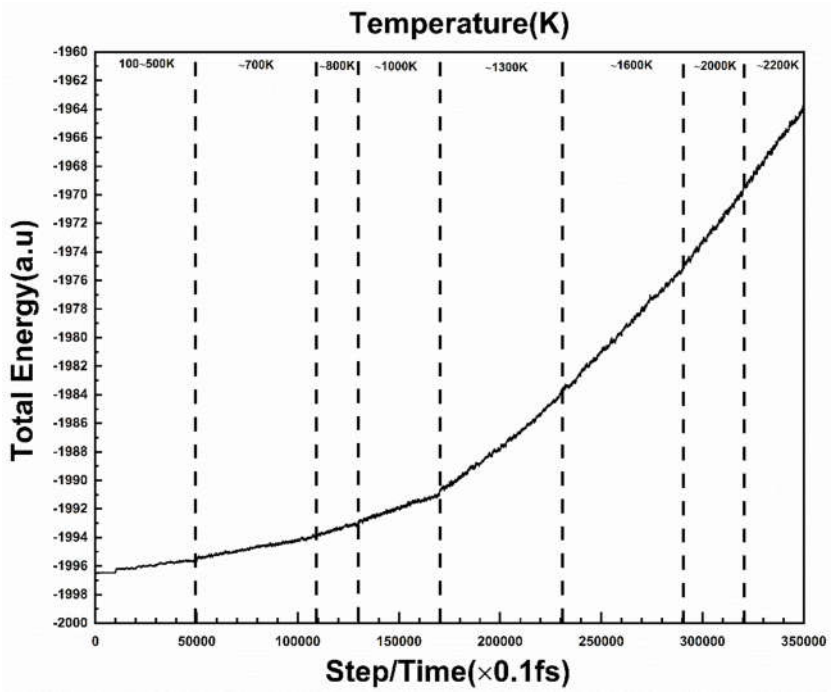

Fig. S8. The relationship between the total energy and the simulation time/temperature of CoCP

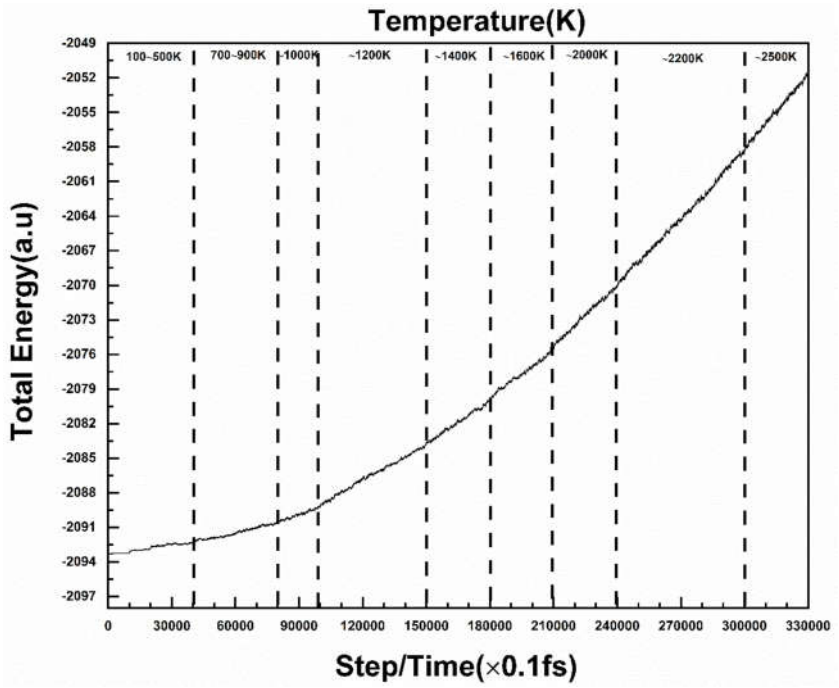

Fig. S9. The relationship between the total energy and the simulation time/temperature of NiCP

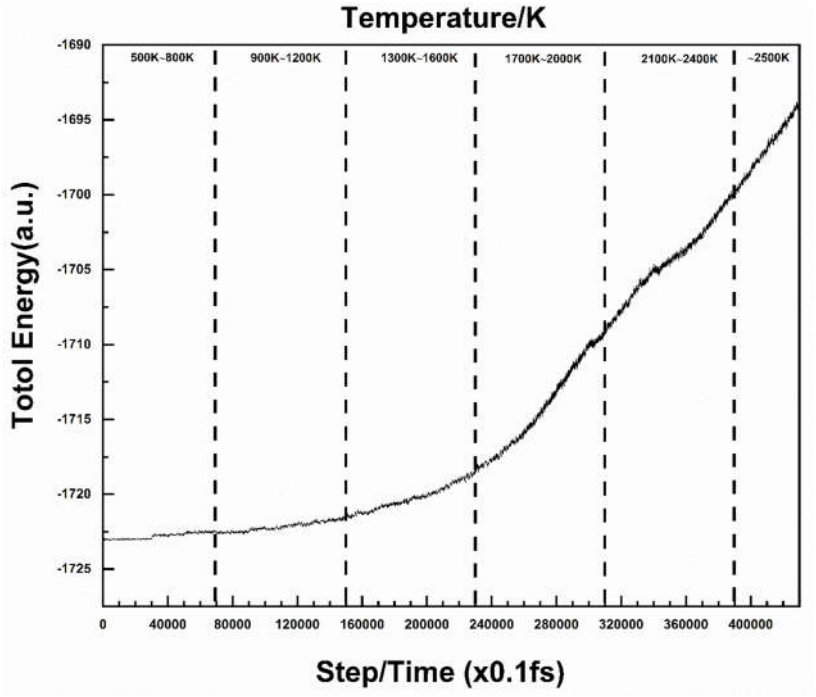

Fig. S10. The relationship between the total energy and the simulation time/temperature of CdCP

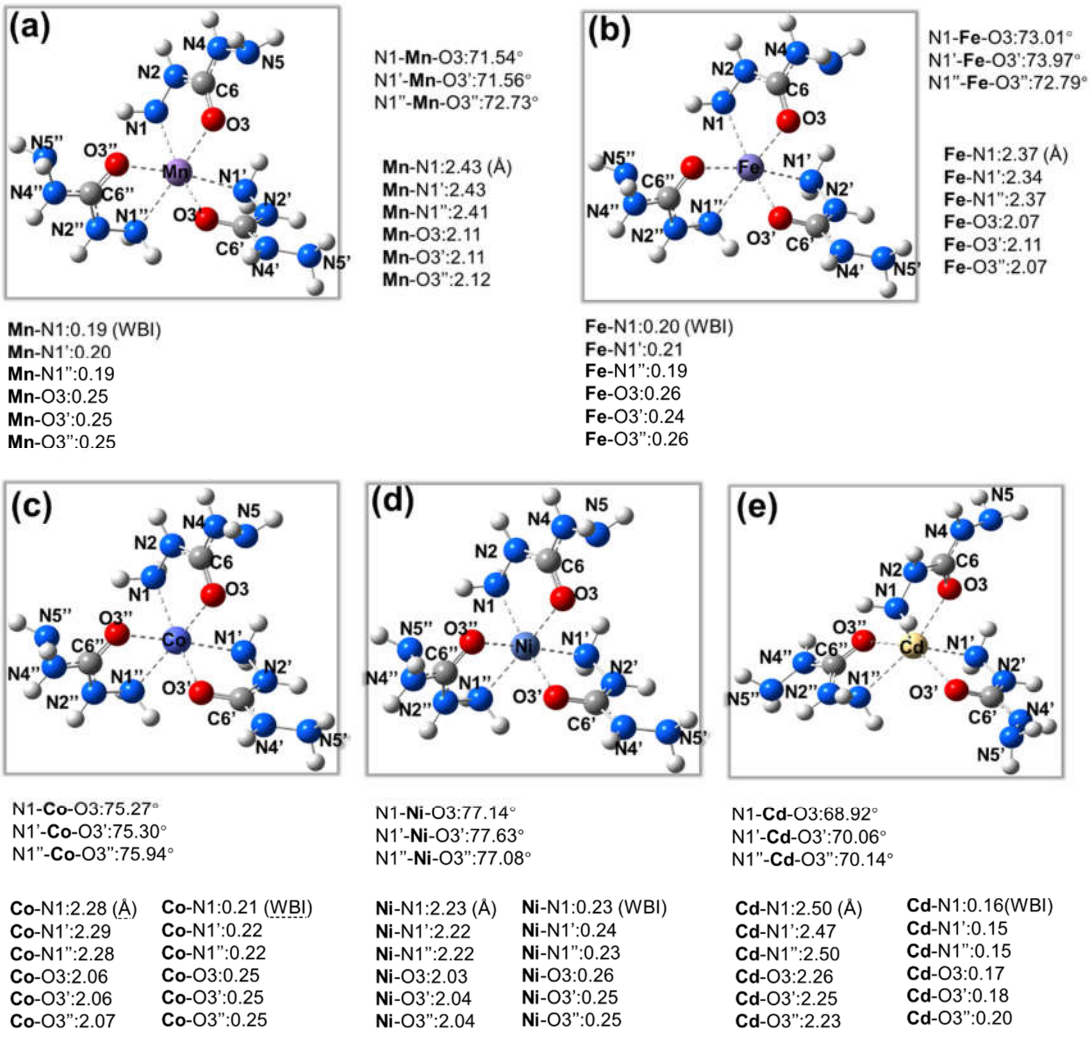

Fig. S11 The molecular structures, parameters and Wiberg bond index of coordinative bonds (WBI) of (a)-(e) $[M(CHZ)_2]^{2+}$ (M^{2+} = Mn^{2+}, Fe^{2+}, Co^{2+}, Ni^{2+}, Zn^{2+} and Cd^{2+}) under the level of m062x/def2tzvp

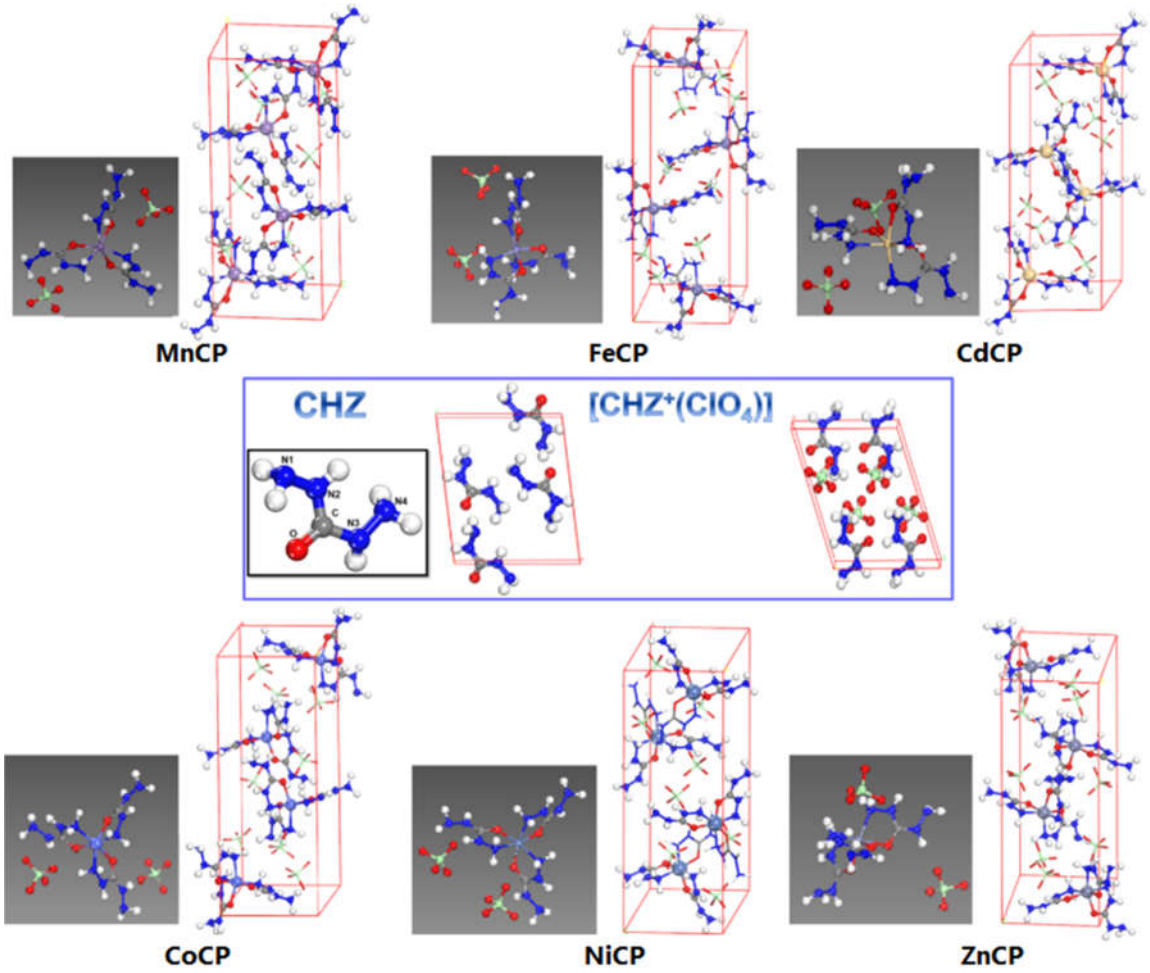

Fig. S12 The optimized crystal structures of CHZ, $[CHZ^{2+}(ClO_4^-)_2]$ and six MCPs (M^{2+} = Mn^{2+}, Fe^{2+}, Co^{2+}, Ni^{2+}, and Cd^{2+})

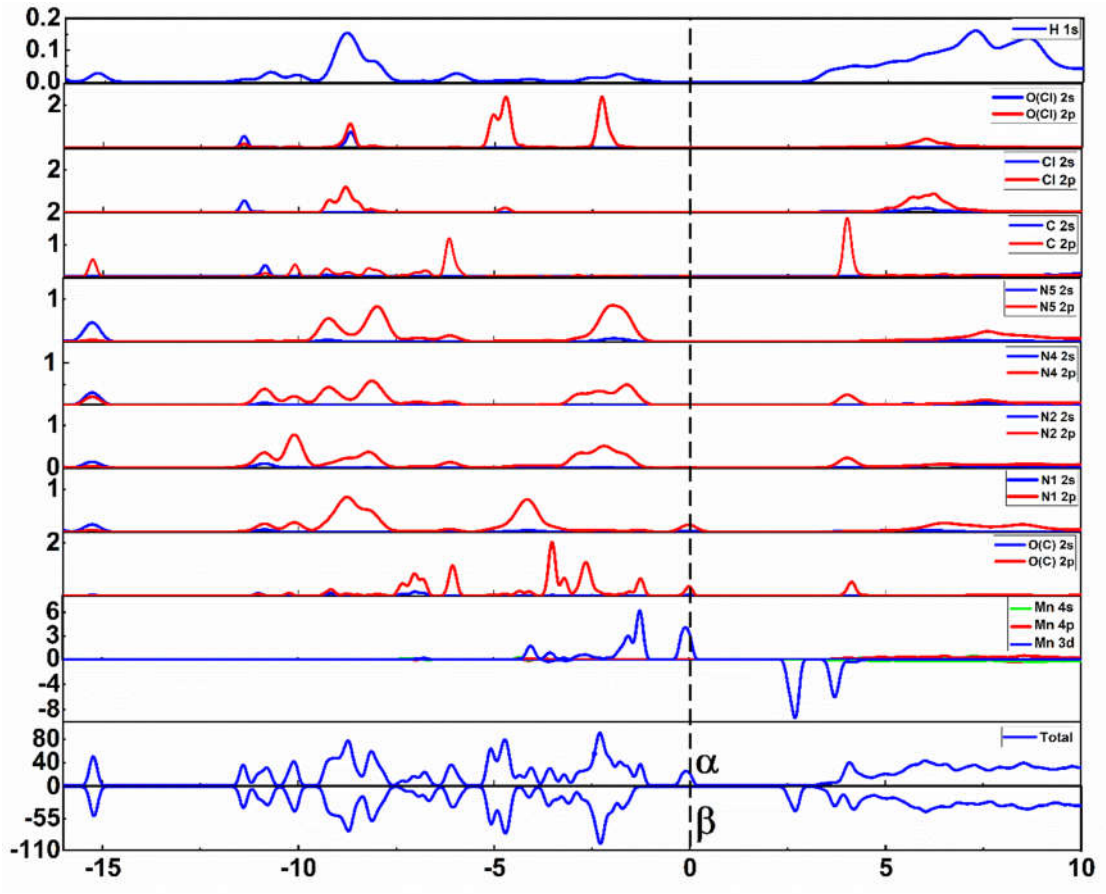

Fig. S13. The density of states (DOS) and partial density of states (pDOS) of MnCP.

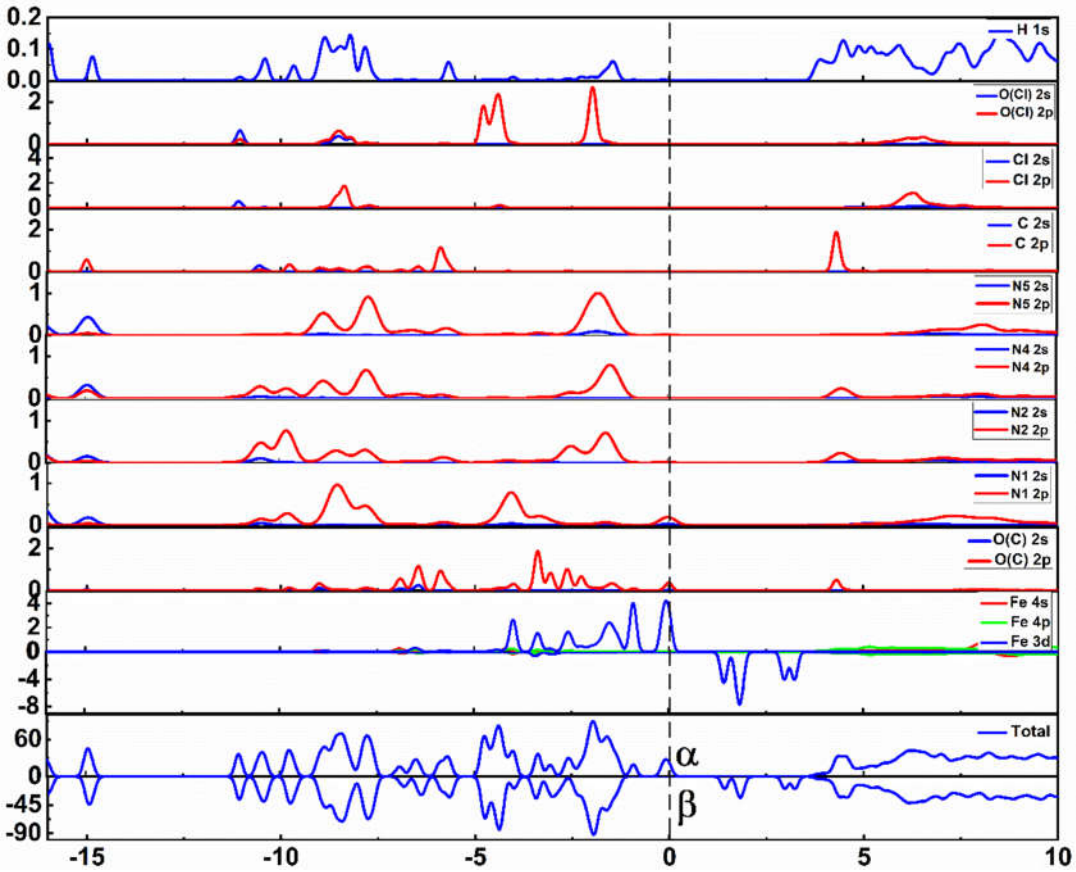

Fig. S14. The density of states (DOS) and partial density of states (pDOS) of FeCP.

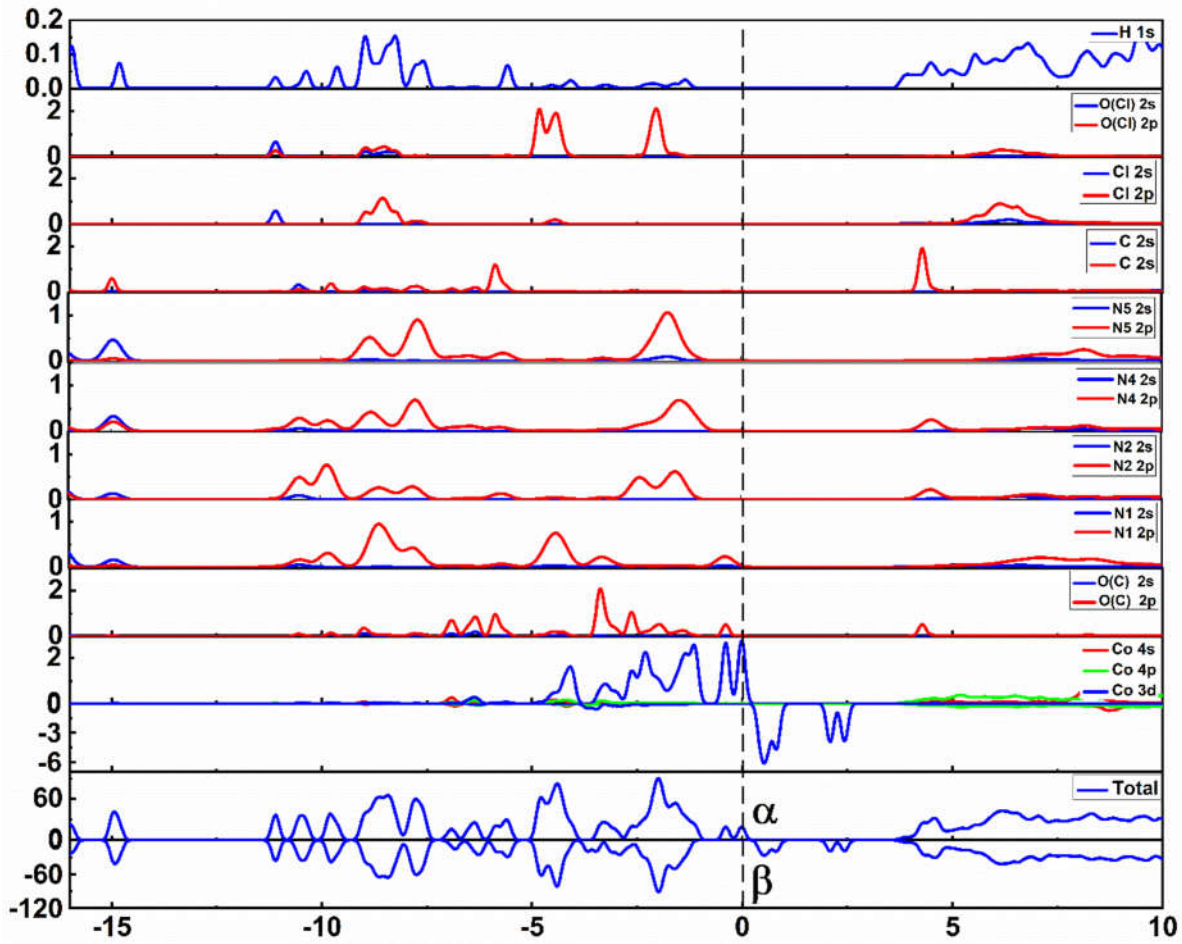

Fig. S15. The density of states (DOS) and partial density of states (pDOS) of CoCP.

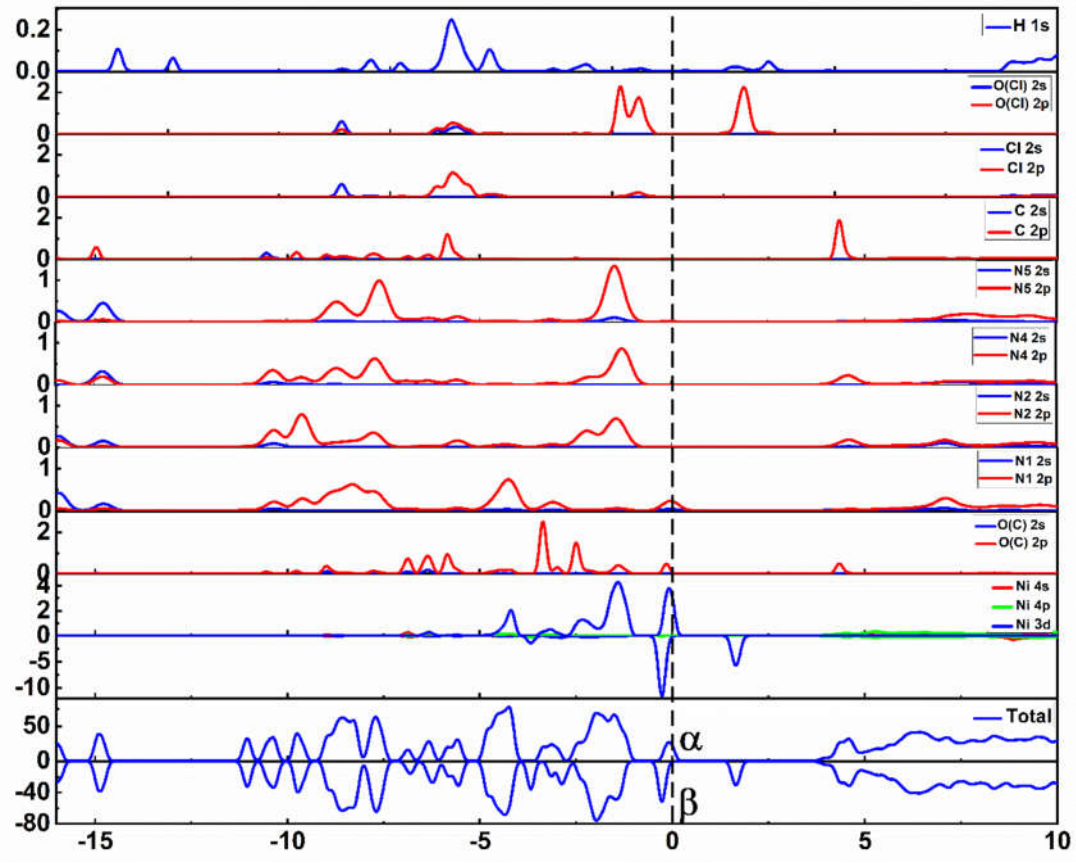

Fig. S16. The density of states (DOS) and partial density of states (pDOS) of NiCP.

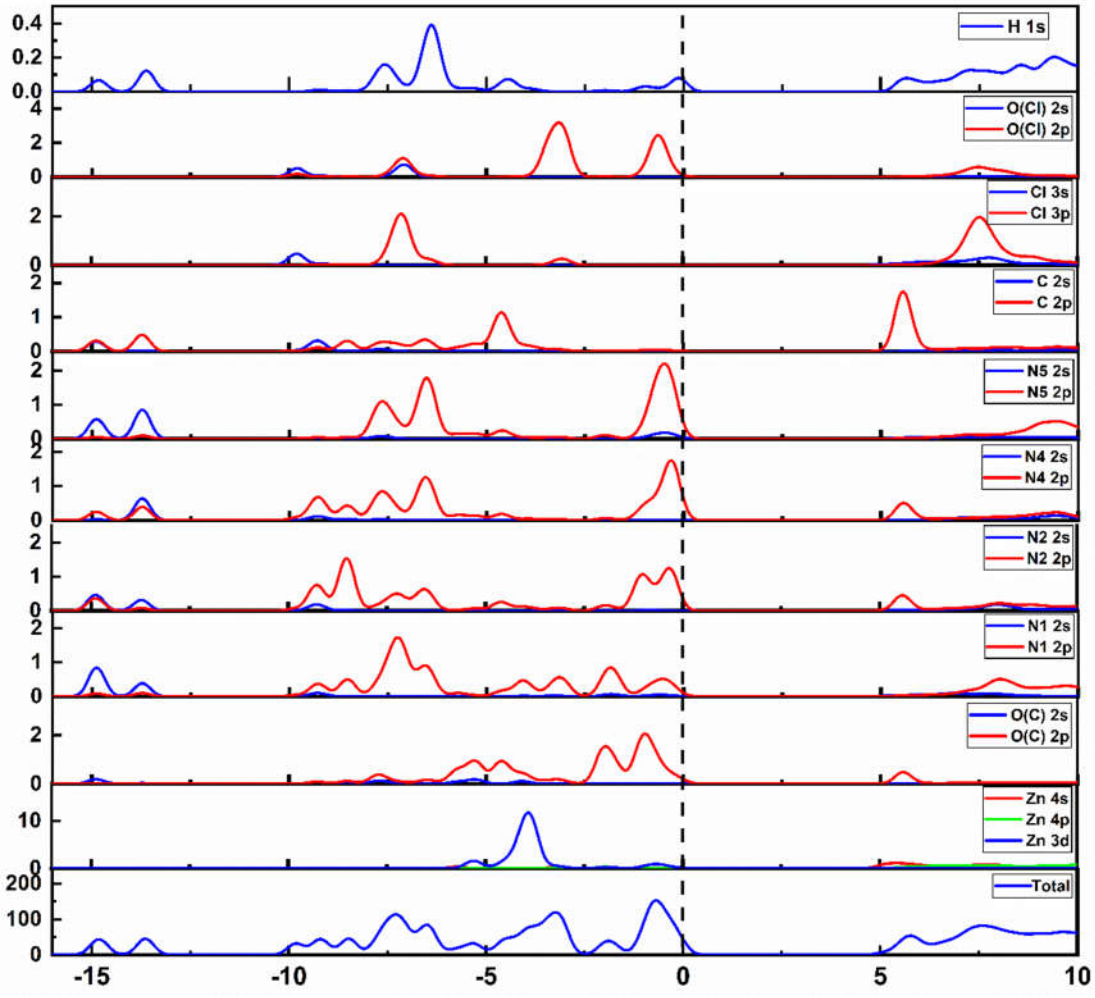

Fig. S17. The density of states (DOS) and partial density of states (pDOS) of ZnCP.

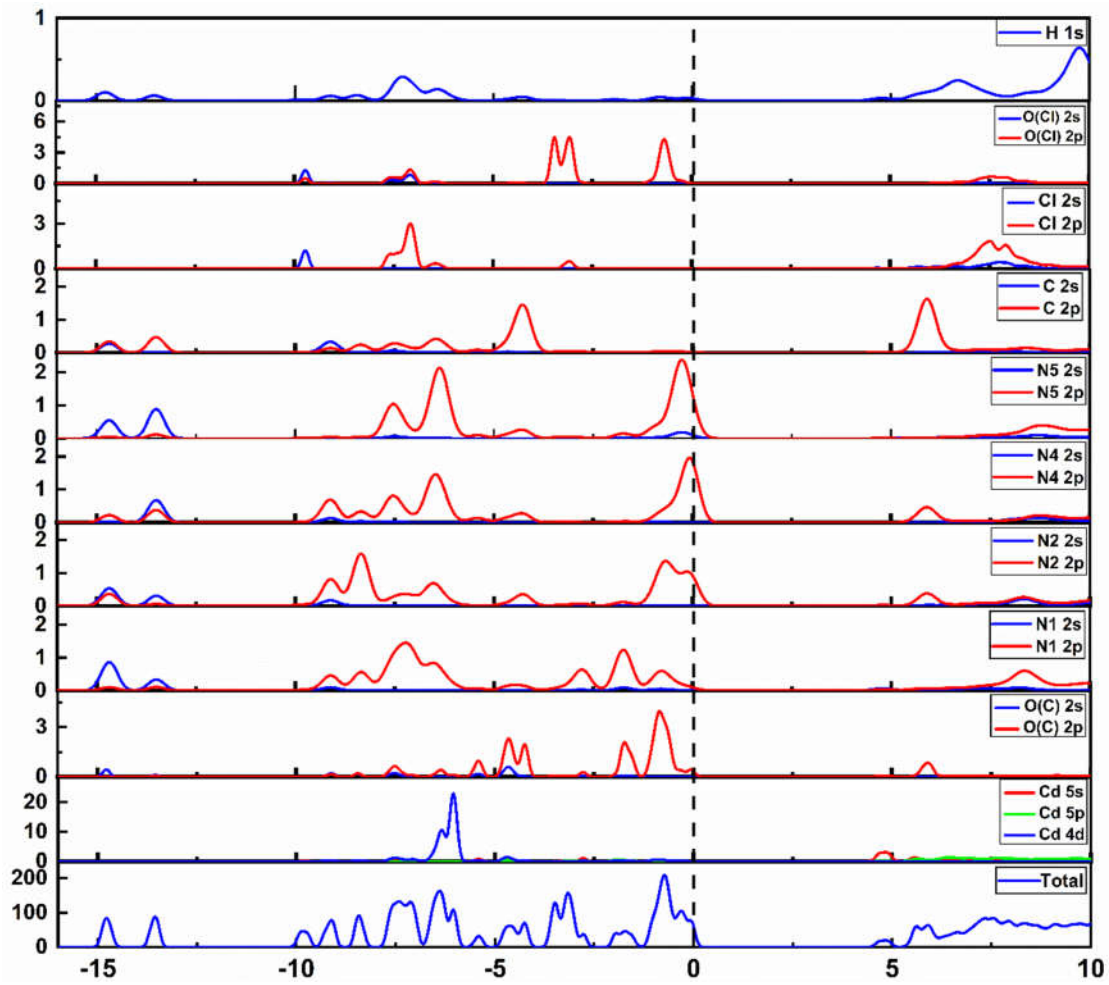

Fig. S18. The density of states (DOS) and partial density of states (pDOS) of CdCP.

The intermolecular interactions among CHZ, M^{2+} and ClO_4^-

In order to understand intermolecular interactions among CHZ, M^{2+} and ClO_4^-, we compare the individual molecular CHZ and the ligand CHZ of MCPs (CHZ(M)) in Fig. S9. In the Hirshfeld surfaces of Fig. 2(a), the red dots represent the distance between molecules is less than the van der Waals distance and therefore suggest the presence of strong intermolecular interactions. In the individual molecular CHZ, most of the red dots located along the surface edges of the plate-like Hirshfeld surface are related to the intermolecular H···H interactions with the percentage of 50.7%, higher than N-H···O (12.2%) and C=O···H (14.9%) in Fig. 2(e). In CHZ(M), the intermolecular H···H interactions decreased drastically, but with obviously increased O···H interactions between CHZ and ClO_4^-.

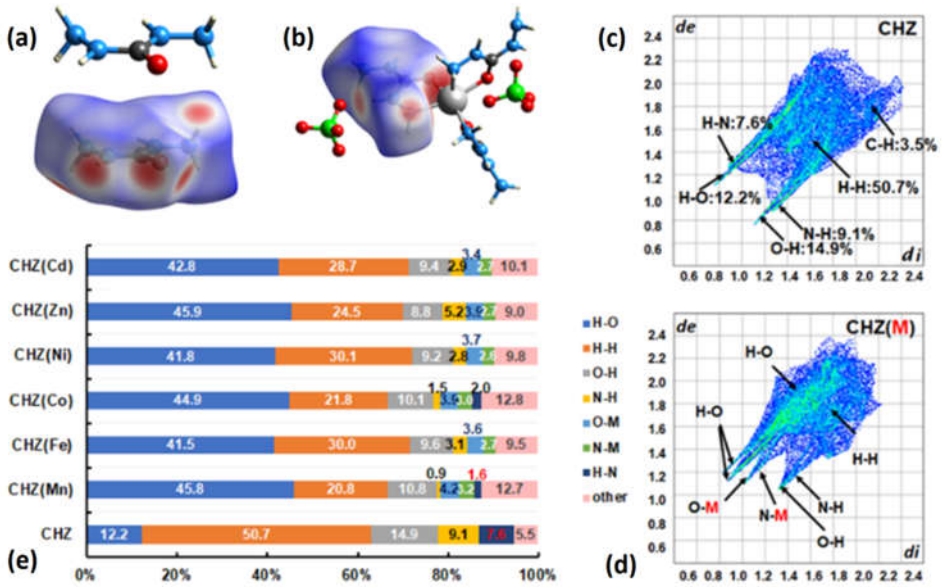

Fig. S19 Molecular structure and Hirshfeld surfaces of individual molecular (a) CHZ and (b) CHZ(M); fingerprint plot of (c) CHZ and (d) CHZ(M); (e) populations of intermolecular interactions of CHZ and CHZ(M).

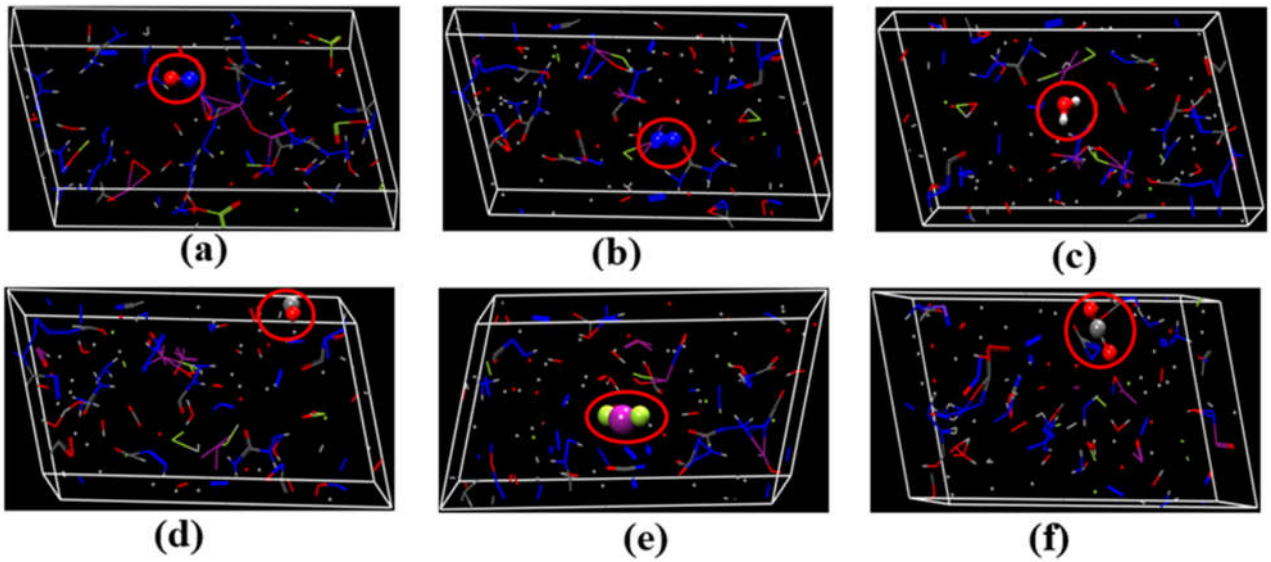

Fig. S20. The snapshots of the typical products of MnCP. (a) the formation of NO at 27.11 ps; (b) the formation of N2 at 33.89 ps; (c) the formation of H2O at 34.46 ps; (d) the formation of CO at 34.84 ps. (e) the formation of $MnCl_2$ at 35.36 ps; (f) he formation of CO2 at 39.46 ps.

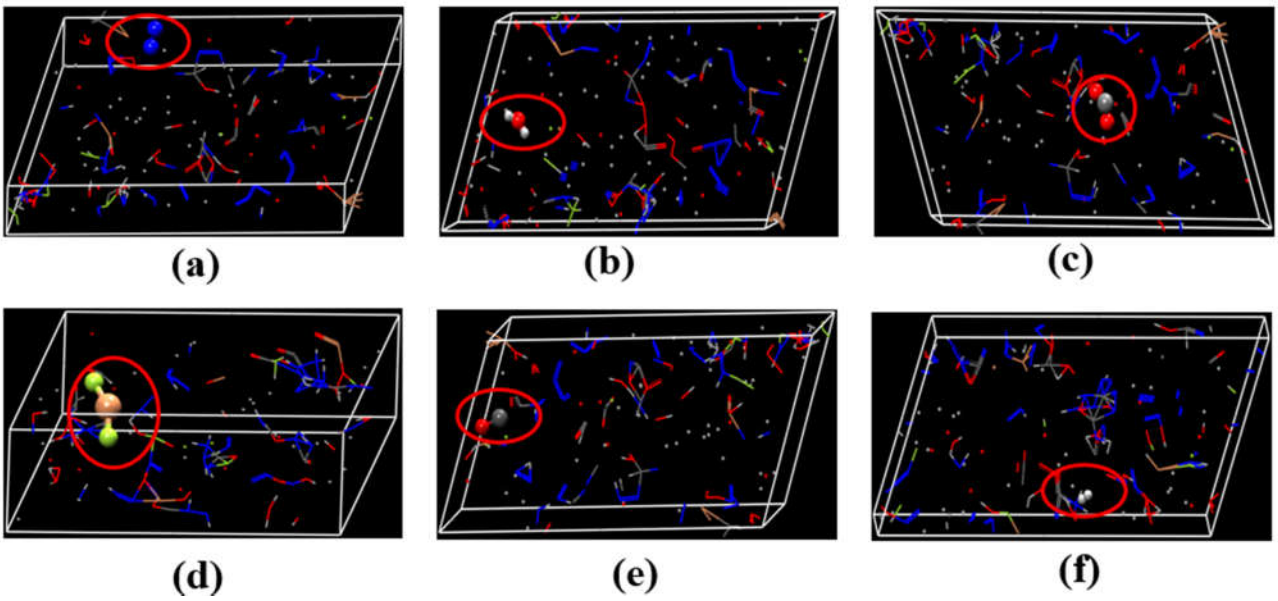

Fig. S21. The snapshots of the typical products of FeCP. (a) the formation of N_2 at 17.47 ps; (b) the formation of H_2O at 23.99 ps; (c) the formation of CO_2 at 25.17 ps; (d) the formation of $FeCl_2$ at 26.88 ps. (e) the formation of

CO at 34.57 ps; (f) the formation of H_2 at 38.08 ps.

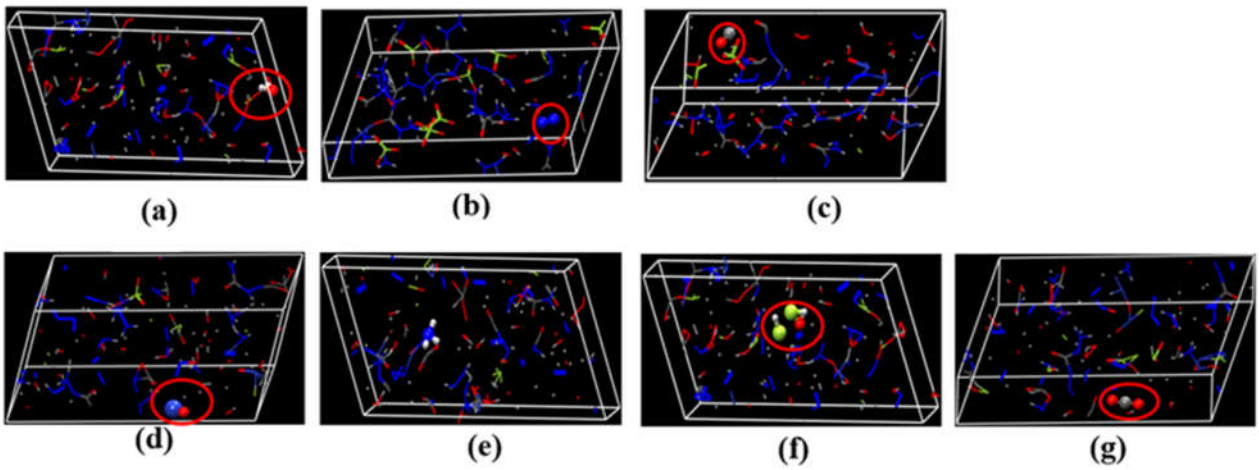

Fig. S22. The snapshots of the typical products of CoCP. (a) the formation of H_2O at 17.62 ps; (b) the formation of N_2 at 19.01 ps; (c) the formation of CO at 22.86 ps; (d) the formation of CoO at 25.49 ps; (e) the formation of NH_3 at 27.41 ps; (f) the formation of HCl and HClO at 28.00 ps; (g) the formation of CO_2 at 32.79 ps.

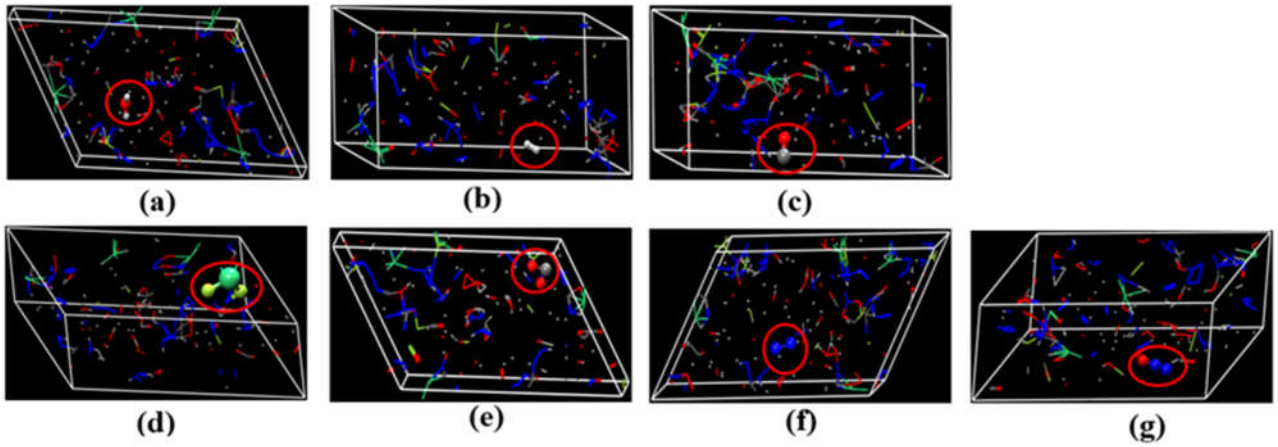

Fig. S23. The snapshots of the typical products of NiCP. (a) the formation of H_2O at 16.05 ps; (b) the formation of H_2 at 20.08 ps; (c) the formation of CO at 24.08 ps; (d) the formation of $NiCl_2$ at 25.40 ps; (e) the formation of CO_2 at 25.81 ps; (f) the formation of and N_2 at 25.81 ps; (g) the formation of N_2O at 26.31 ps.

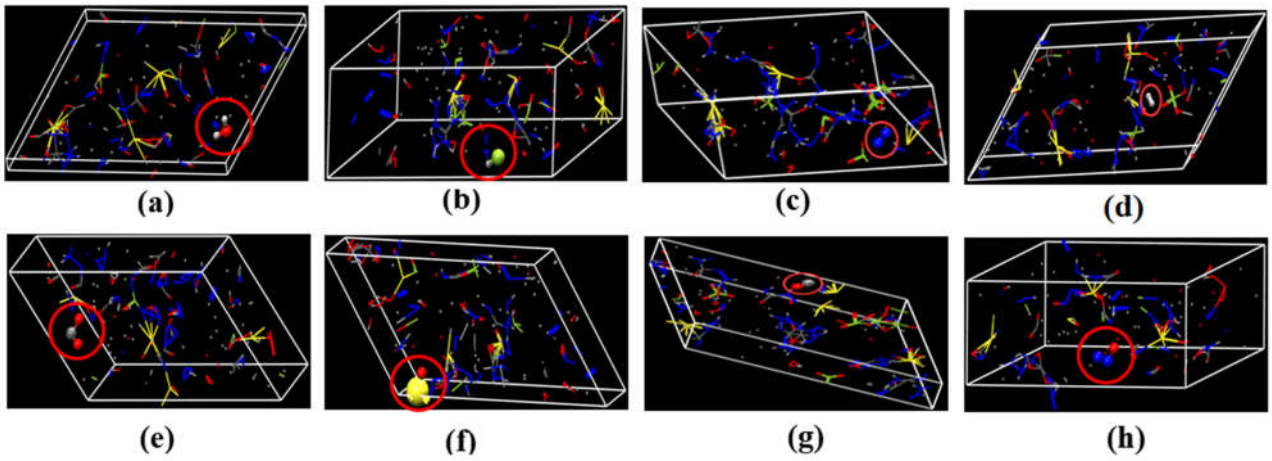

Fig. S24. The snapshots of the typical products of CdCP. (a) the formation of H_2O at 26.30 ps; (b) the formation of HCl at 26.86 ps; (c) the formation of N_2 at 27.55 ps; (d) the formation of H_2 at 27.55 ps; (e) the formation of CO_2 at 27.55 ps; (f) the formation of and CdO at 33.38 ps; (g) the formation of CO at 33.83 ps; (g) the formation of N_2O at 36.76 ps.

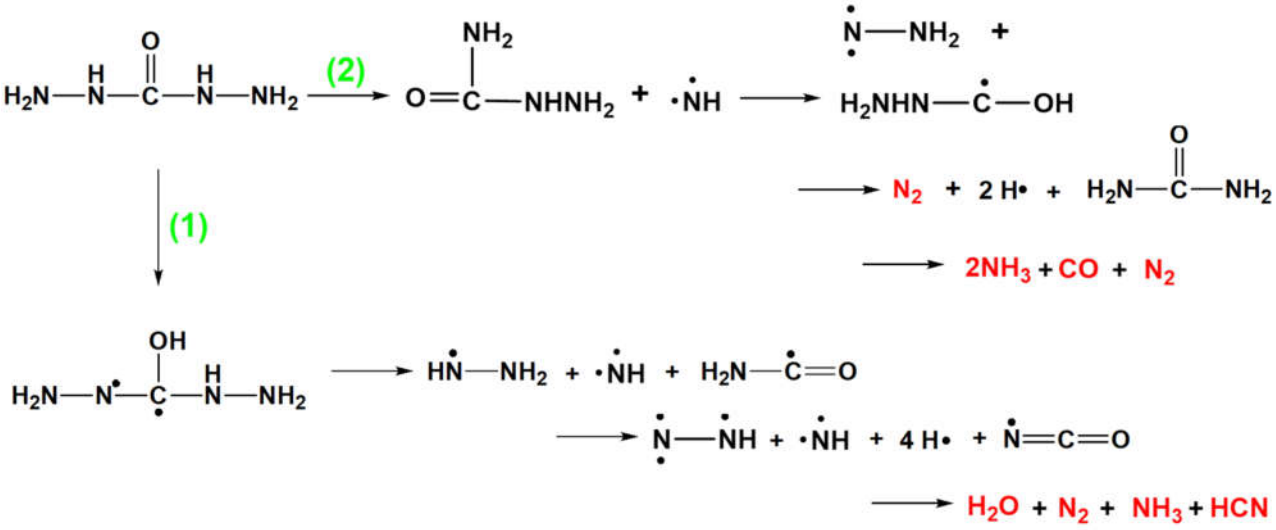

Scheme S1. The decomposition pathways of CHZ

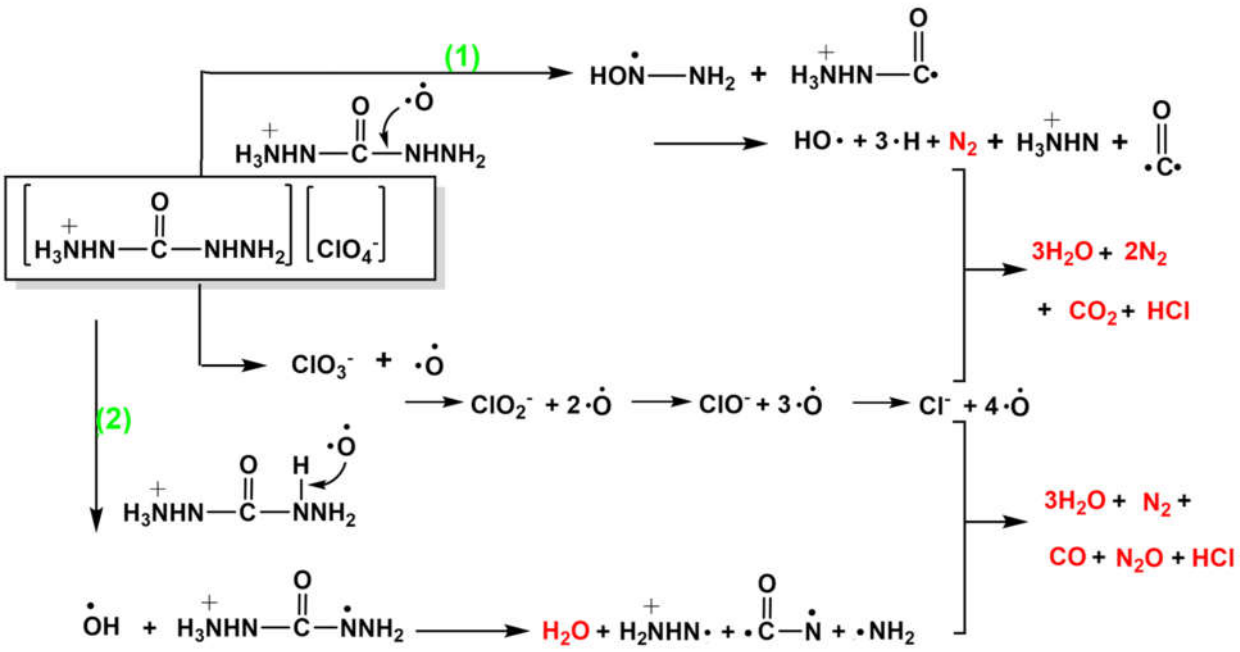

Scheme S2. The decomposition pathways of CHZCP

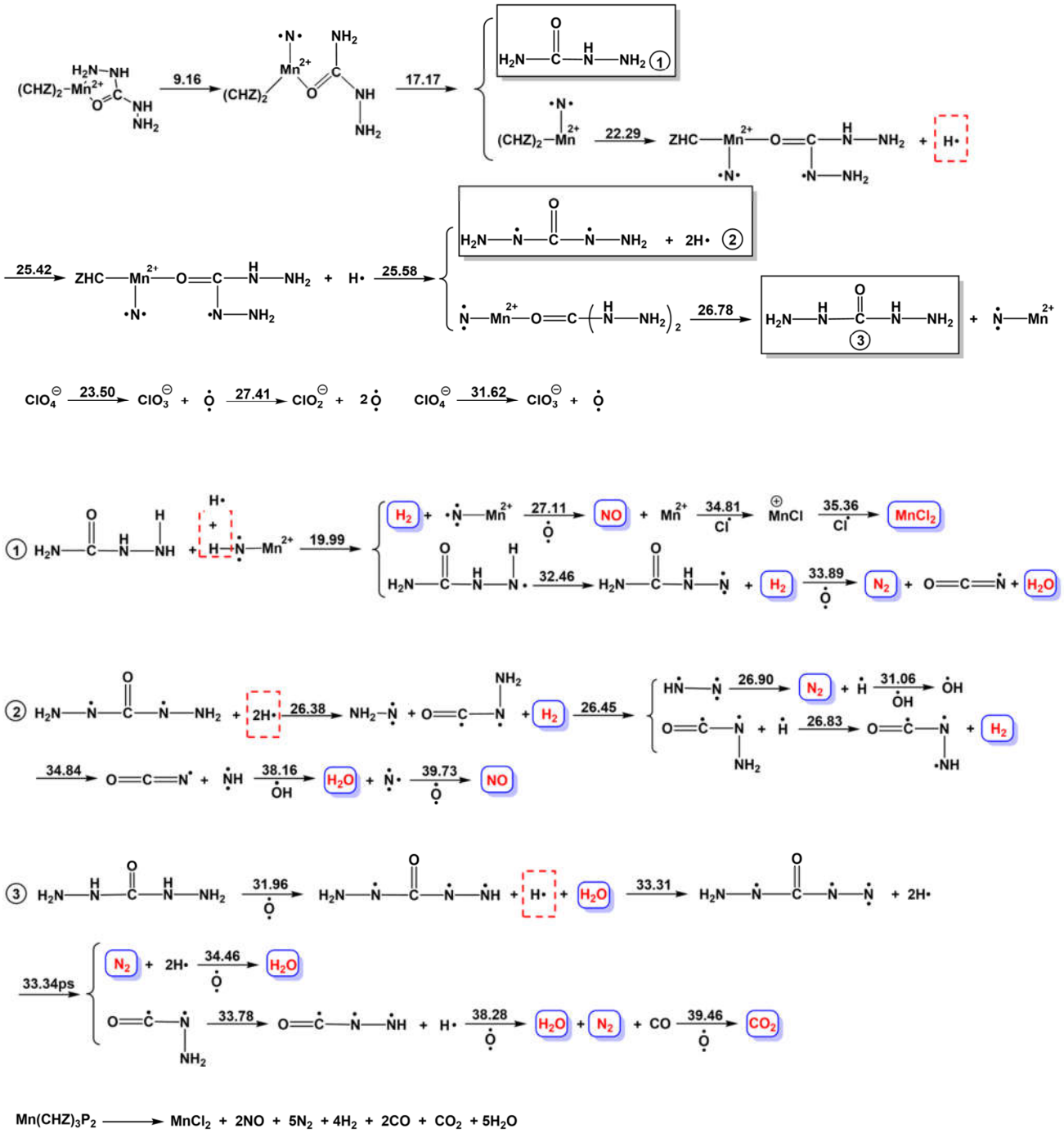

Scheme S3. The decomposition pathways of MnCP

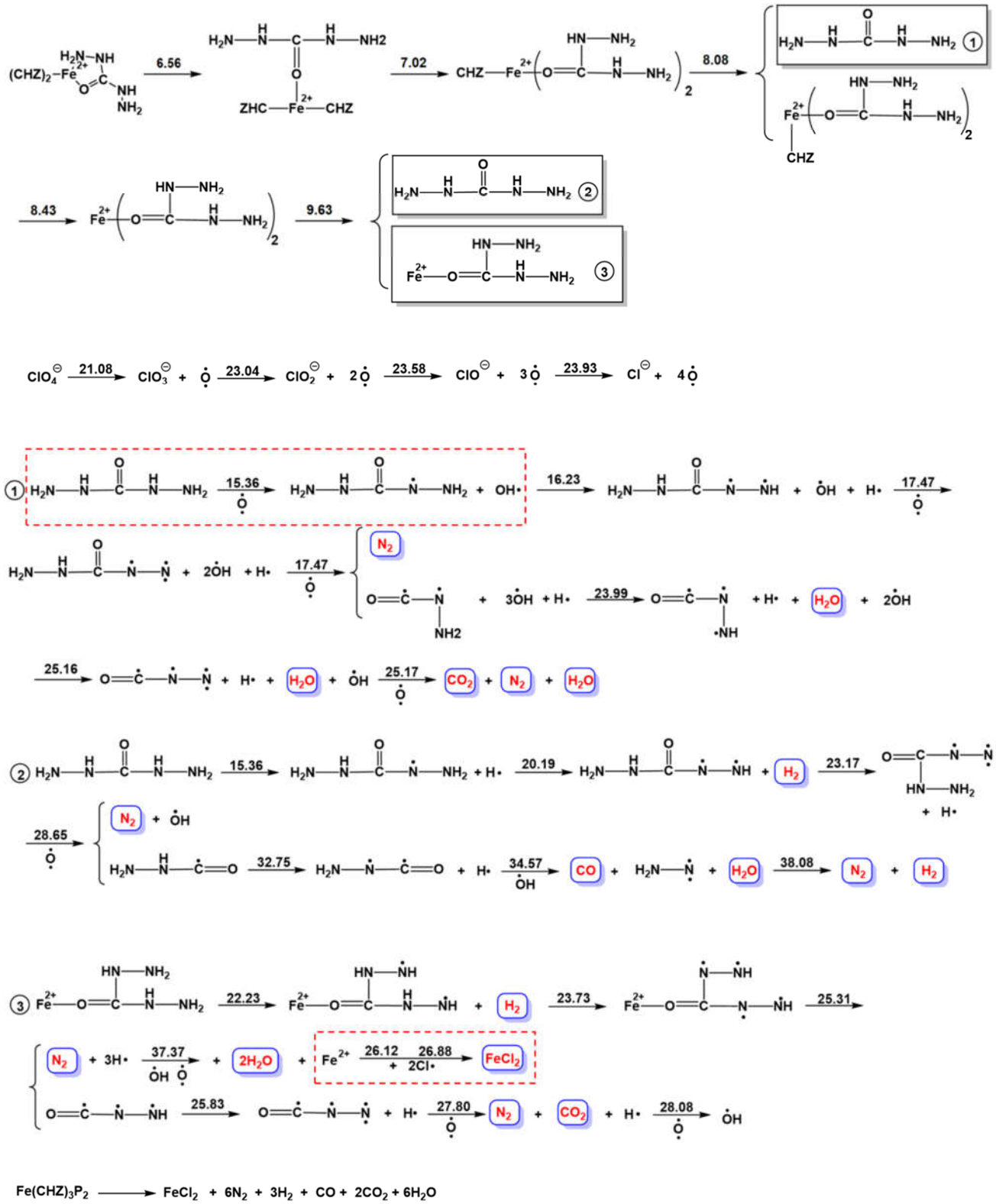

Scheme S4. The decomposition pathways of FeCP

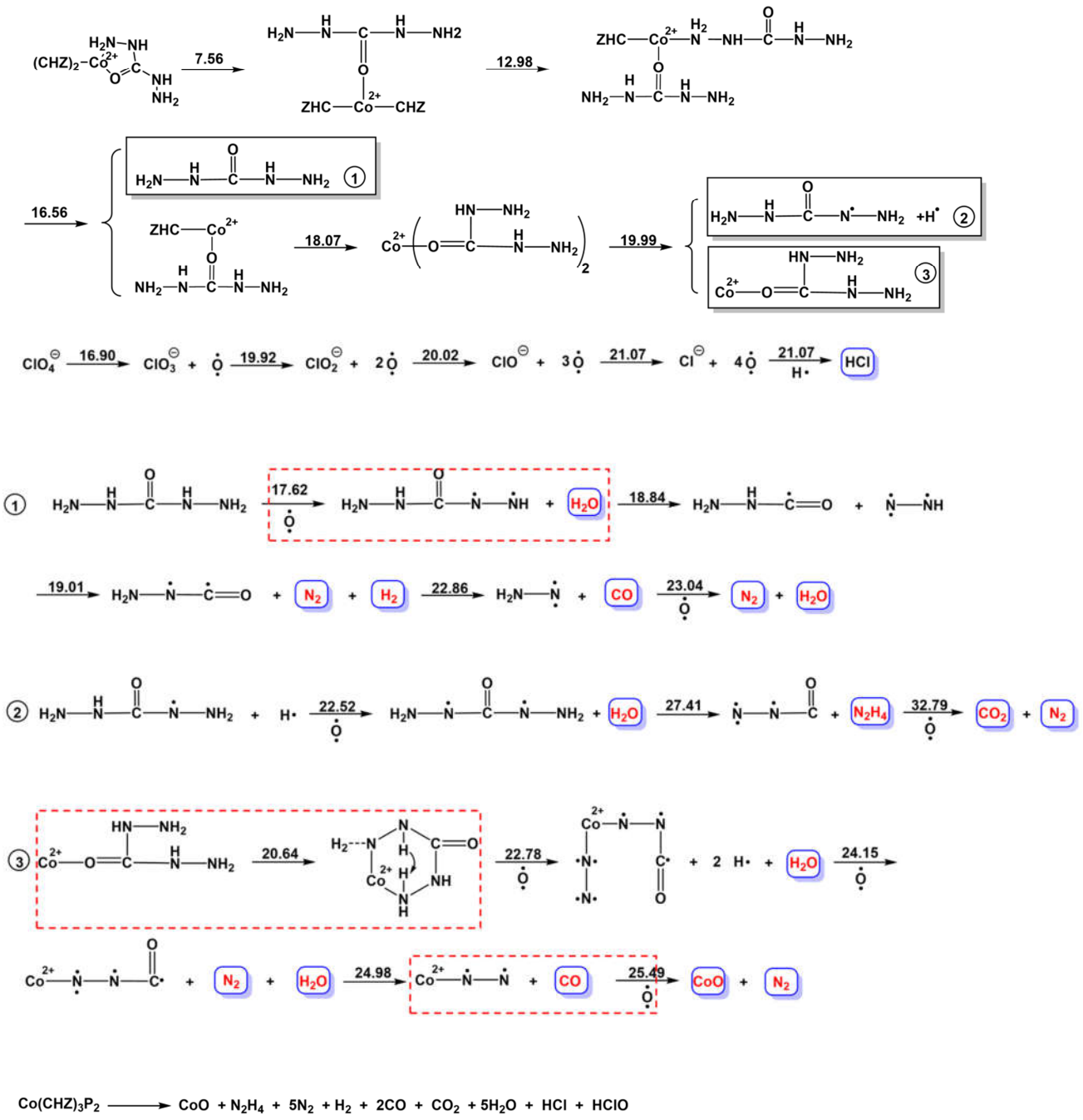

Scheme S5. The decomposition pathways of CoCP

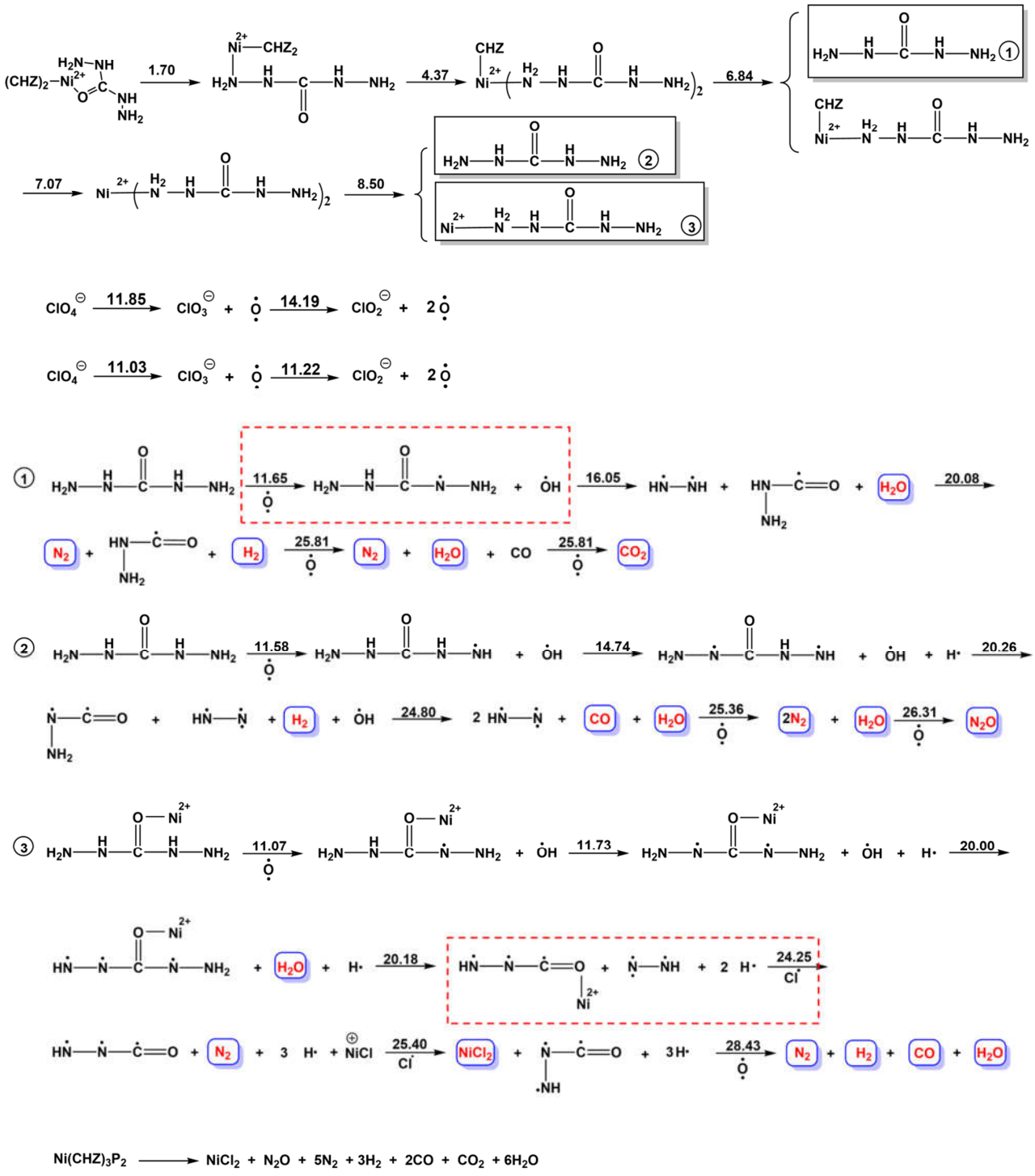

Scheme S6. The decomposition pathways of NiCP

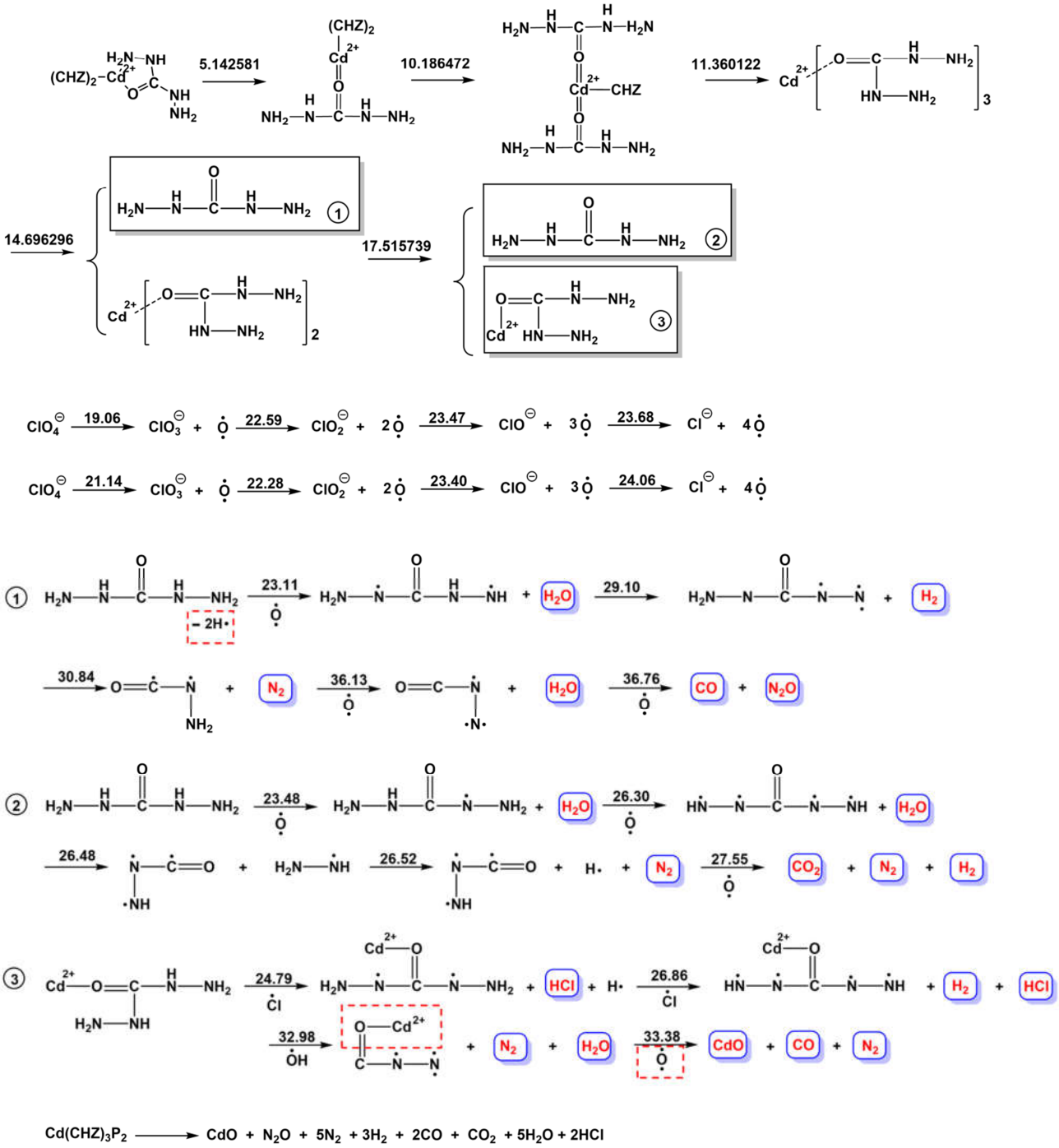

Scheme S7. The decomposition pathways of CdCP

Table S1~Table S5. The Cartesian coordinates of $[M(CHZ)_2]^{2+}$ (M^{2+} = Mn^{2+}, Fe^{2+}, Co^{2+}, Ni^{2+} and Cd^{2+}) of the optimized structure under the level of m062x/def2tzvp.

Table S1. The Cartesian coordinates of $[Mn(CHZ)_2]^{2+}$ of the optimized structure under the level of m062x/deftzvp.

Atom	x	y	z
O	1.007455	-1.530340	0.557955
N	2.004472	-0.321340	-1.633428
N	2.809018	-1.036015	-0.739827
N	3.054265	-2.213680	1.210195
N	4.424325	-2.245236	0.970367
C	2.237923	-1.585012	0.357070
H	3.815935	-1.062590	-0.836487
H	2.317461	0.647278	-1.660463
H	2.105967	-0.715901	-2.564639
H	2.637755	-2.606677	2.044110
H	4.748483	-3.202133	0.885460
H	4.926897	-1.780906	1.718734
N	-1.237270	-2.121181	-1.339918
O	-2.063883	-0.194272	0.310746
N	-1.156433	1.774610	-1.663180
O	0.751077	1.661497	0.198764
C	-2.753035	-1.222267	0.254756
C	0.264678	2.774019	-0.042627
N	0.624212	3.894528	0.596765
N	1.584914	3.836910	1.597271
N	-3.865680	-1.407322	0.976890
N	-4.289851	-0.415245	1.850711
N	-0.673609	2.925394	-1.029444
N	-2.412123	-2.241280	-0.591389
H	-1.201271	3.780859	-1.123054
H	-2.127548	1.614361	-1.400683
H	-1.104068	1.902131	-2.669461
H	0.201834	4.777656	0.342187
H	1.185364	4.109513	2.486943
H	2.368438	4.435232	1.367074
H	-1.449220	-2.257704	-2.324174
H	-0.567168	-2.829347	-1.046228
H	-2.891943	-3.128905	-0.577636
H	-4.391758	-2.266047	0.882142
H	-4.262755	-0.749718	2.806215
H	-5.226555	-0.114311	1.611998
Mn	-0.128165	-0.114372	-0.533282

Table S2. The Cartesian coordinates of $[Fe(CHZ)_2]^{2+}$ of the optimized structure under the level of m062x/def2tzvp.

Atom	x	y	z
O	0.726109	-1.535697	0.590975
N	1.825407	-0.549930	-1.647181
N	2.533472	-1.387968	-0.779009
N	2.654467	-2.531034	1.204801
N	3.993853	-2.785566	0.926855
C	1.920270	-1.800222	0.357364
H	3.523591	-1.558981	-0.897284
H	2.292485	0.353786	-1.695001
H	1.823125	-0.956529	-2.578694
H	2.210765	-2.826418	2.064518
H	4.160071	-3.783479	0.860368
H	4.587734	-2.389390	1.646967
N	-1.397767	-1.876477	-1.395802
O	-2.056730	0.045813	0.299566
N	-0.990043	1.976230	-1.536298
O	0.987704	1.527627	0.169167
C	-2.813603	-0.935325	0.252628
C	0.656540	2.710660	-0.002029
N	1.229913	3.737972	0.635261
N	2.244101	3.498927	1.553117
N	-3.921159	-1.051631	0.994173
N	-4.261245	-0.039822	1.882330
N	-0.324192	3.028558	-0.899798
N	-2.544774	-1.965247	-0.602853
H	-0.717314	3.956542	-0.953613
H	-1.961425	1.942840	-1.231594
H	-0.962202	2.119098	-2.541499
H	0.923388	4.682840	0.444030
H	1.956530	3.788867	2.479942
H	3.086759	3.988866	1.279341
H	-1.654726	-1.929312	-2.377746
H	-0.770260	-2.646374	-1.173669
H	-3.106585	-2.802370	-0.639270
H	-4.497163	-1.879291	0.913707
H	-4.229235	-0.379846	2.835793
H	-5.184091	0.317732	1.668994
Fe	-0.177369	-0.020357	-0.560765

Table S3. The Cartesian coordinates of $[Co(CHZ)_2]^{2+}$ of the optimized structure under the level of m062x/def2tzvp.

Atom	x	y	z
O	-0.988265	-1.461408	-0.490433
N	-1.981160	-0.120795	1.608705
N	-2.805650	-0.777016	0.687400
N	-3.049645	-1.949029	-1.266972
N	-4.427870	-1.841419	-1.109466
C	-2.228653	-1.392262	-0.370841
H	-3.812966	-0.687536	0.720858
H	-2.209172	0.871622	1.608445
H	-2.157134	-0.492587	2.538600
H	-2.625810	-2.395455	-2.069695
H	-4.850051	-2.760158	-1.034099
H	-4.836611	-1.341829	-1.891499
N	1.031149	-2.076953	1.399415
O	1.911756	-0.238456	-0.312514
N	1.216527	1.554254	1.735458
O	-0.638513	1.606176	-0.173760
C	2.513709	-1.319986	-0.296259
C	-0.020047	2.658094	0.032994
N	-0.216385	3.784894	-0.661984
N	-1.147676	3.802647	-1.691615
N	3.550223	-1.605888	-1.093918
N	3.992726	-0.659547	-2.008540
N	0.899524	2.733766	1.047564
N	2.156149	-2.297440	0.594829
H	1.542493	3.508948	1.115217
H	2.178551	1.288462	1.533067
H	1.122092	1.718064	2.733950
H	0.301831	4.620478	-0.424615
H	-0.691314	3.988545	-2.576280
H	-1.858479	4.500510	-1.510533
H	1.284820	-2.217663	2.373513
H	0.296431	-2.736489	1.149680
H	2.522716	-3.235444	0.530114
H	4.015667	-2.500531	-1.015570
H	3.875123	-1.000649	-2.954766
H	4.964249	-0.432189	-1.836725
Co	0.094160	-0.127926	0.664537

Table S4. The Cartesian coordinates of $[Ni(CHZ)_2]^{2+}$ of the optimized structure under the level of m062x/def2tzvp.

Atom	x	y	z
O	0.976511	-1.397690	0.533537
N	1.929271	-0.114873	-1.614058
N	2.774131	-0.734577	-0.685360
N	3.050548	-1.840203	1.303787
N	4.425656	-1.720567	1.127820
C	2.213854	-1.321018	0.400033
H	3.779640	-0.633254	-0.734020
H	2.152885	0.877949	-1.653525
H	2.090040	-0.516844	-2.534232
H	2.640563	-2.260129	2.127806
H	4.858699	-2.636071	1.079277
H	4.835890	-1.190048	1.888489
N	-0.972367	-2.022282	-1.432660
O	-1.842274	-0.251242	0.351791
N	-1.168128	1.460874	-1.785983
O	0.583707	1.574939	0.213978
C	-2.438186	-1.333994	0.306651
C	-0.042124	2.611167	-0.037258
N	0.092463	3.749389	0.653304
N	0.969036	3.798545	1.728821
N	-3.457584	-1.657742	1.111379
N	-3.890734	-0.748568	2.067184
N	-0.906325	2.658612	-1.104492
N	-2.094744	-2.275508	-0.631830
H	-1.566390	3.414878	-1.210546
H	-2.137216	1.186458	-1.634188
H	-1.021144	1.607154	-2.780945
H	-0.430383	4.570716	0.379141
H	0.463919	3.979679	2.587548
H	1.671760	4.511433	1.577476
H	-1.229531	-2.130802	-2.409979
H	-0.235319	-2.689392	-1.210330
H	-2.437476	-3.223385	-0.580196
H	-3.919537	-2.551482	1.006323
H	-3.753986	-1.122514	2.998240
H	-4.866349	-0.521492	1.920185
Ni	-0.082122	-0.131769	-0.671176

Table S5. The Cartesian coordinates of $[Cd(CHZ)_2]^{2+}$ of the optimized structure under the level of m062x/def2tzvp.

Atom	x	y	z
O	2.062363	-0.884412	-0.708648
N	2.080081	1.032815	1.223851
N	3.244217	0.522423	0.652269
N	4.308487	-0.893622	-0.797981
N	5.518326	-0.389691	-0.331515
C	3.151223	-0.437508	-0.300446
H	4.162345	0.848792	0.926149
H	2.111954	0.916323	2.232881
H	1.991594	2.027778	1.029710
H	4.254703	-1.610658	-1.509536
H	6.039511	0.040772	-1.087233
H	6.073900	-1.127480	0.086986
N	-0.792052	0.859844	-2.017859
O	-0.850290	1.914346	0.484055
N	-0.693727	-1.276026	2.085111
O	-1.508427	-1.489075	-0.479670
C	-1.499326	2.476220	-0.407769
C	-1.994190	-2.266886	0.345592
N	-2.928871	-3.179283	0.040417
N	-3.392996	-3.271384	-1.265301
N	-2.221968	3.588489	-0.196366
N	-2.288577	4.134926	1.078029
N	-1.590753	-2.258496	1.658348
N	-1.517794	2.005016	-1.692408
H	-2.115165	-2.757931	2.361560
H	-1.163294	-0.599992	2.684622
H	0.052066	-1.717403	2.615332
H	-3.231311	-3.845274	0.738975
H	-4.400176	-3.170990	-1.284433
H	-3.122965	-4.156592	-1.677213
H	-0.152364	1.055496	-2.781687
H	-1.415756	0.098621	-2.281480
H	-2.136285	2.399900	-2.385009
H	-2.681430	4.045209	-0.972872
H	-3.249645	4.173554	1.393990
H	-1.882377	5.062464	1.087639
Cd	0.150389	-0.057615	0.074485

Table S6. The syngony, symmetry, band gaps, cell parameters, selected atomic charges, typical bond lengths and bond angles of crystal CHZ, [$CHZ^{+}(ClO_4^{-})$] and MCPs.

	CHZ	[$CHZ^{+}(ClO_4)$]	MnCP	FeCP	CoCP	NiCP	ZnCP	CdCP
syngony	monoclinic	monoclinic	monoclinic	monoclinic	monoclinic	monoclinic	monoclinic	monoclinic
Space group	P2/C	P21/C	P21/N	P21/N	P21/N	P21/C	P21/N	P21/C
Band gap (eV)	5.18	5.18	4.11 (3.33)[1]	3.66 (2.74)[1]	3.70 (1.73)[1]	3.77 (1.79)[1]	4.91	4.56
a (Å)	9.05 (3.72)[2]	11.15 (10.00)[2]	11.04 (10.20)[2]	10.54 (10.07)[2]	10.47 (10.05)[2]	10.46 (9.97)[2]	10.51 (10.00)[2]	10.53 (10.28)[2]
b (Å)	4.66 (8.82)	7.41 (8.42)	8.74 (8.59)	8.82 (8.46)	8.72 (8.54)	8.76 (8.56)	8.72 (8.43)	8.97 (8.62)
c (Å)	10.65 (11.96)	9.41 (21.21)	21.29 (21.41)	22.10 (21.19)	22.18 (21.43)	22.61 (21.43)	22.17 (21.22)	23.53 (21.36)
α (°)	90.00	90.00	90.00	90.00	90.00	90.00	90.00	90.00
β (°)	96.93	109.40	97.73	99.57	99.75	107.50	99.89	109.39
γ (°)	90.00	90.00	90.00	90.00	90.00	90.00	90.00	90.00

[1.] The value in bracket is the band gap of spin-down electrons;

[2.] The values in brackets are the experimental results.

Table S7. The temperature of ions (T_{ion}), kinetic energies of virtual electrons (e_{kinc}) and the total electronic energies (e_{tot}) of MCPs (M^{2+} = Mn^{2+}, Fe^{2+}, Co^{2+}, Ni^{2+} and Cd^{2+}).

	MnCP	FeCP	CoCP	NiCP	CdCP
Tions (K)	60.83	11.70	51.59	16.50	124.35
ekinc (a.u)	1.99×10^{-1}	1.19×10^{-2}	1.04×10^{-1}	6.81×10^{-3}	1.46×10^{-2}
etot (a.u)	-1842.57	-1923.89	-1996.54	-2091.19	-1723.48